Magnetic force microscopy and x-ray scattering study of 70×550 nm² pseudo-spin-valve nanomagnets

F. J. Castaño,[a] Y. Hao, S. Haratani, and C. A. Ross[b]
Department of Materials Science and Engineering, Massachusetts Institute of Technology, Cambridge, Massachusetts 02139

B. Vögeli and Henry I. Smith
Department of Electrical Engineering and Computer Science, Massachusetts Institute of Technology, Cambridge, Massachusetts 02139

C. Sánchez-Hanke and C.-C. Kao
National Synchrotron Light Source, Brookhaven National Laboratory, Upton, New York 11073

X. Zhu and P. Grütter
Center for the Physics of Materials, Department of Physics, McGill University, 3600 University St., Montreal, Quebec H3A 2T8, Canada

(Presented on 14 November 2002)

The room-temperature magnetic properties of large area arrays of 70×550 nm² nanoelements made from a NiFe 6 nm/ Cu 3 nm/ Co 4 nm multilayer stack have been investigated using magnetic force microscopy (MFM), alternating gradient magnetometry (AGM), and scattering experiments using synchrotron radiation. MFM measurements on individual elements show square major and minor loops, while the collective magnetization reversal, measured from both AGM and elementally specific hysteresis loops obtained from synchrotron scattering experiments, show a wide distribution of switching fields and interaction fields, due to the variability between the elements. © *2003 American Institute of Physics.* [DOI: 10.1063/1.1558076]

I. INTRODUCTION

The magnetic properties of lithographically defined multilayered magnetic solids with three dimensions in the nanometer range have recently drawn significant attention.[1,2] Issues such as how the magnetization reversal is affected by the shape and reduced dimensions of these nanomagnets are of considerable interest for the development of high-density magnetoresistive random access memory (MRAM) devices.[3–5] Nanomagnets being explored as memory cells are composed of at least two magnetic layers sandwiching a nonmagnetic insulating or metallic spacer. Future high-density MRAM devices will require layered magnetic elements with thicknesses below a few tens of nanometers and in-plane dimensions in the sub-100 nm regime.

The overall magnetic behavior of these nanomagnets is governed by shape anisotropy, resulting in an easy magnetization axis parallel to the longer in-plane dimension of the structure. For reduced aspect ratios, as a result of magnetostatic coupling, the magnetization of the magnetic layers has been shown to align antiparallel at remanence.[6,7] From a device point of view, high-density arrays composed of single-domain, magnetically identical elements displaying abrupt magnetization reversal are desirable.

Many nanomagnet arrays produced to date[3,4] have been made using serial lithography processes such as electron-beam lithography, and thus the arrays fabricated typically cover areas of a few hundred square microns. This does not allow for simultaneous probing of both local and wide-area magnetic properties. With this in mind, we have produced large-area (square cm) arrays of NiFe/Cu/Co pseudo-spin-valve (PSV) elongated elements with aspect ratios up to 20 and widths ranging between 65 nm and 100 nm.[6–10] These simple PSV elements can be used as models to investigate the behavior of sub-100 nm magnetic multilayer elements. In the present article, we present a detailed study of a sample composed of 70×550 nm² NiFe/Cu/Co PSV nanomagnets, characterized using magnetic force microscopy (MFM), alternating gradient magnetometry (AGM), and scattering experiments using synchrotron radiation.

II. EXPERIMENT

The nanomagnet array was patterned from a sputtered NiFe (6 nm)/ Cu (3 nm)/ Co (4 nm)/ Cu (4 nm) thin film, using a combination of interference lithography, reactive ion etching, and ion milling (for processing details see Ref. 9). Room-temperature hysteresis loops and minor loops were measured in a piece of the array containing $\sim 10^9$ nanomagnets using AGM. Minor loops were obtained by saturating the sample in an applied field and then measuring the magnetic moment on increasing the field from different reversing fields (H_R), which were applied in the opposite direction to that of the saturating field. The MFM measurements were performed over a 3 μm×3 μm area using a high-resolution custom-built vacuum MFM system,[11] using as tips silicon cantilevers coated with a 25 nm thick sputtered CoPtCr alloy. Images presented in this work were taken at remanence, to

[a]Electronic mail: fer@mit.edu
[b]Author to whom correspondence should be addressed; electronic mail: caross@mit.edu
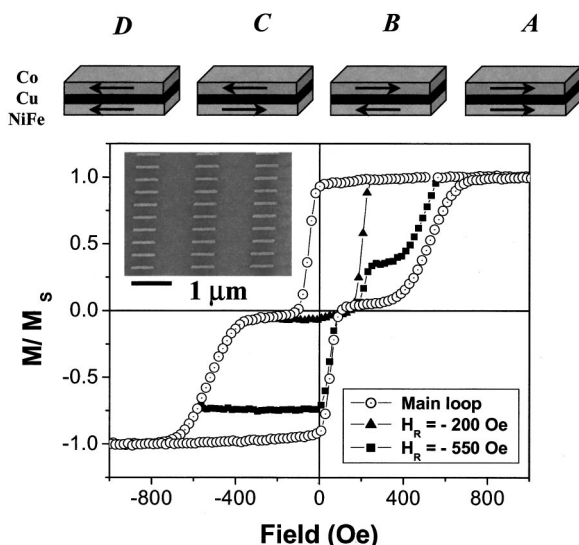
FIG. 1. Room-temperature hysteresis loop and minor loop measurements corresponding to a 70×550 nm^2 NiFe/Cu/Co PSV nanomagnet array. The reversing fields of the minor loops are -200 Oe (filled triangles) and -550 Oe (filled squares). The inset shows a scanning electron micrograph of part of the sample. A schematic representation of the four possible orientations of the magnetization of an element is also depicted.

FIG. 2. Sequential MFM images mapping the magnetization reversal over a $3 \ \mu m \times 3 \ \mu m$ area of the sample investigated. MFM images taken at remanence: (a) after saturating in 800 Oe and after subsequently applying (b) -65 Oe; (c) -97 Oe; (d) -405 Oe; (e) -550 Oe; and (f) -650 Oe.

reduce the perturbing effects resulting from the interaction between the tip and the external applied field.

Using circularly polarized light from the X-13A beamline at the National Synchrotron Light Source, both reflectivity and magnetic circular dichroism patterns were measured for these arrays. An elliptically polarizing wiggler provided linear or modulated elliptically polarized light switching with 22 Hz between the left- and right-hand polarization of the x-ray beam. The beamline, with two spherical gratings of 800 and 1600 grooves/mm, works in an energy range between 250 eV and 1.8 keV, which covers the L absorption edges corresponding to transition metal elements. An electromagnet mounted on the sample holder supplies a magnetic field up to 1.0 kOe, along the sample surface. Under these conditions, the beamline setup allows both detector and sample scans together with energy and magnetic field dependence measurements. Here, we discuss the magnetic parameters deduced from elementally specific hysteresis loops, obtained from the signal difference close to the L3 absorption edge of the Co, Ni, and Fe present in the sample, and measured as a function of the applied magnetic field.

III. RESULTS AND DISCUSSION

AGM hysteresis measurements reveal the distinct switching of each of the magnetic layers (NiFe and Co) in the patterned elements at different applied fields (see Fig. 1). The four possible different magnetic states (A, B, C, and D) of the patterned elements are also schematically depicted in Fig. 1. The NiFe soft layers reverse over a range of applied fields centered at 115 Oe, while the Co hard layers reverse over a range of fields centered at 410 Oe.

The hysteresis loop shape can be understood as a superposition of the hysteresis of a large number of patterned elements with a distribution of switching fields for both the
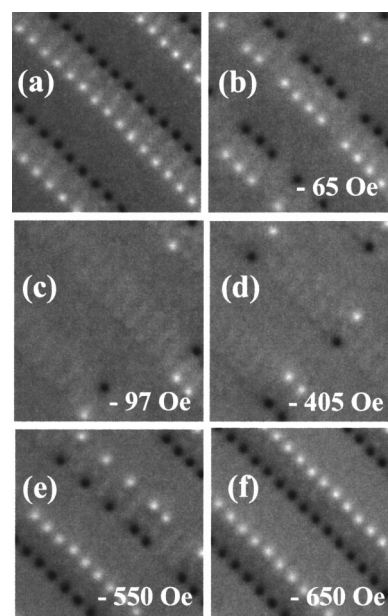
hard (Co) and soft (NiFe) magnetic layers. Due to the relatively large spacing between the elements in the arrays, magnetostatic interactions between the PSV elements may be neglected, and the hysteresis loops can be simulated by treating each PSV element as a coupled pair of rectangular magnetic films (Co and NiFe), interacting through exchange and magnetostatic coupling.[7] Within each PSV element, the Co exerts a field on the NiFe (H_{hs}) and vice versa (H_{sh}).[9] The coercive field of the NiFe layers $H_{C,NiFe}$ can be measured from the minor loop, and the coupling field H_{hs} can be obtained as the offset from zero-applied field of the NiFe minor loop. For the experimental data shown in Fig. 1, $H_{C,NiFe}$ and H_{hs} are 125 Oe and 60 Oe, respectively.

Figure 2 shows a sequence of MFM images taken on applying a saturating field [Fig. 2(a)] and after subsequent application of an opposite reversing field [Figs. 2(b)–2(f)]. The MFM images show bright and dark contrast close to the patterned ends of the elements, suggesting single domain states for each of the magnetic layers. In the saturated state [Fig. 2(a)], all elements are in the A state and, on increasing the reverse field [Figs. 2(b)–2(f)], B states are initially formed eventually becoming D states for higher reverse fields. The B states have very weak MFM contrast. Remanence hysteresis loops were calculated based on the MFM data from an area containing 460 ± 10 patterned elements, and compared to the remanence loops measured using AGM in arrays containing $\sim 10^9$ patterned elements.[13] Experimentally deduced averaged parameters from the MFM remanence measurements (switching fields, interaction field, and coercive field for the NiFe layers) are in excellent agreement with those deduced from AGM measurements.

Furthermore, single element hysteresis and minor loops were measured using MFM, by positioning the tip at one end of the patterned element and monitoring the cantilever fre-
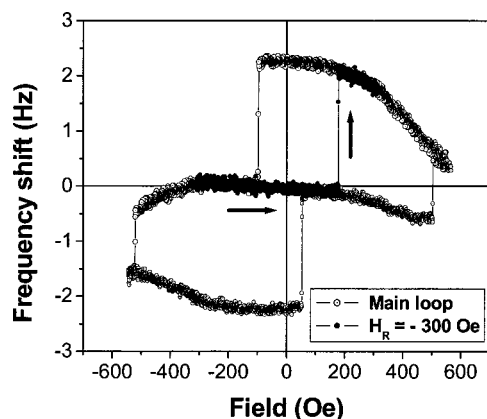
FIG. 3. Hysteresis loop and minor loop corresponding to a single 70 ×550 nm² NiFe/Cu/Co element. The reversing field used to obtain the minor loop is −300 Oe.

quency shift while sweeping the external field. The cantilever frequency shift is proportional to the force gradient between the tip and the sample, thus providing a measure of the magnetic moment. Such measurements (see Fig. 3) reveal square hysteresis loops for individual patterned elements with abrupt switching at well-defined field values. The coercive field $H_{C,\text{NiFe}}$ and the interaction field H_{hs} deduced from the individual element shown in Fig. 3 are 137 Oe and 40 Oe, respectively. Measurements on different patterned elements show the same overall shapes of the hysteresis loops, but a distribution of switching fields consistent with AGM data.

In comparison, elementally specific hysteresis loops obtained using synchrotron scattering[12] provide values of the average coercive field for the Ni and Co within the patterned structures. Synchrotron data are presented in Fig. 4. In these data, the reversal of the Ni and Fe occurs at identical fields,
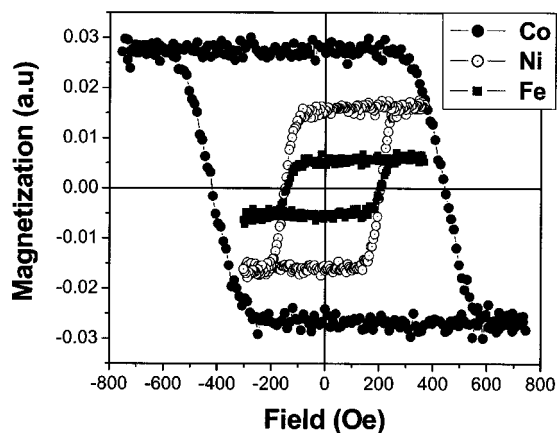
as expected, while the Co reverses at a higher field. The Ni and Fe loops are both offset from zero, by 40 Oe, as a result of the interaction field H_{hs}. All three elements show a distribution of switching fields consistent with AGM data. The average coercive field for the Ni was 120 Oe and for the Co was 410 Oe, which is similar to the results obtained from AGM.

Overall, the experimental values deduced for $H_{C,\text{NiFe}}$ and H_{hs} from wide-area AGM and x-ray measurements are in good agreement, and show a distribution of switching fields, while MFM measurements on individual nanomagnets show square loops with a range of switching fields, particularly for H_{hs}. This fact reinforces a picture in which wide-area magnetic properties of the array can be interpreted as a superposition of the magnetic behavior of a large number of individual nanomagnets. Individual patterned elements show well-defined switching and interacting fields, while the ensemble displays distributions for the switching fields for both layers, as well as for the interaction field between layers. The switching field distributions can be ascribed to irregularities in element edge shape, resulting from the lithographic processing; to microstructural variations between the polycrystalline elements; or to the effect of ion-milling which leads to a disordered region at the edges of the elements.[10,13] To control the variability, careful control of both the magnetic material (e.g., the choice of lower anisotropy or cubic materials) and the lithographic and patterning processes are required.

ACKNOWLEDGMENTS

FIG. 4. Elementally specific hysteresis loops, deduced from magnetic circular dichroism measurements, for the array of 70×550 nm² NiFe/Cu/Co nanomagnets.

[1] S. P. Li, W. S. Lew, J. A. C. Bland, L. Lopez-Diaz, M. Natali, A. A. F. Vaz, and Y. Chen, Nature (London) **415**, 600 (2002).

[2] T. Gerrits, H. A. M. van den Berg, J. Hohlfeld, L. Bar, and T. Rasing, Nature (London) **418**, 509 (2002).

[3] J. M. Daughton, A. V. Pohm, R. T. Fayfield, and C. H. Smith, J. Phys. D **32**, R169 (1999); S. Tehrani, E. Chen, M. Durlam, M. DeHerrera, J. M. Slaughter, J. Shi, and G. Kerszykowsky, J. Appl. Phys. **85**, 5822 (1999).

[4] S. S. P. Parkin, K. P. Roche, M. G. Samant, P. M. Rice, R. B. Beyers, R. E. Scheuerlein, E. J. O'Sullivan, S. L. Brown, J. Bucchigano, D. W. Abraham, Y. Lu, M. Rooks, P. L. Trouilloud, R. A. Wanner, and W. J. Gallagher, J. Appl. Phys. **85**, 5828 (1999).

[5] J. G. Zhu and Y. F. Zheng, Top. Appl. Phys. **83**, 289 (2002).

[6] F. J. Castaño, Y. Hao, C. A. Ross, B. Vögeli, H. I. Smith, and S. Haratani, IEEE Trans. Magn. **37**, 2073 (2001).

[7] T. L. Hylton, M. A. Parker, K. R. Coffey, J. K. Howard, R. Fontana, and C. Tsang, Appl. Phys. Lett. **67**, 1154 (1995).

[8] F. J. Castaño, Y. Hao, C. A. Ross, B. Vögeli, H. I. Smith, and S. Haratani, Appl. Phys. Lett. **79**, 1504 (2001).

[9] B. Vögeli, H. I. Smith, F. J. Castaño, Y. Hao, S. Haratani, and C. A. Ross, J. Vac. Sci. Technol. B **19**, 2753 (2001).

[10] F. J. Castaño, Y. Hao, C. A. Ross, B. Vögeli, H. I. Smith, and S. Haratani, J. Appl. Phys. **91**, 7317 (2002).

[11] P. Grütter, Y. Liu, P. LeBlanc, and U. Dürig, Appl. Phys. Lett. **7**, 279 (1997).

[12] C. Sánchez-Hanke and C.-C. Kao, J. Magn. Magn. Mater. **226**, 1803 (2001).

[13] F. J. Castaño, S. Haratani, Y. Hao, C. A. Ross, and H. I. Smith, Appl. Phys. Lett. **81**, 2809 (2002).